Joint inversion of navigation and resistivity using a fixed transmitter and a towed receiver array: a transient marine CSEM model study

Andrei Swidinsky* and R. Nigel Edwards

Department of Physics, University of Toronto, Toronto ON, M5S 1A7, Canada. E-mail: aswidinsky@ifm-geomar.de

SUMMARY

A typical marine controlled-source electromagnetic system consists of an electric dipole transmitter and one or more electric dipole receivers. The objective of a survey is to determine the seafloor resistivity by recording the electromagnetic transients, which diffuse through the earth from the transmitter to the receivers. Accurate knowledge of system geometry is crucial for proper interpretation; errors in the position and orientation of the transmitter and/or the receivers propagate into errors in the predicted seafloor resistivity. We show theoretically that for certain multireceiver set-ups and crustal electrical profiles that the geometry and the seafloor resistivity may be determined independently. A specific example is an experiment proposed in association with NEPTUNE Canada. Here, we have already deployed an electric dipole transmitter with a known orientation in a known location. A cabled streamer of receivers may be towed by a survey vessel in the vicinity of the transmitter on a known heading. For this configuration, an eigenparameter analysis of two seafloor models consisting of (1) a halfspace and (2) a resistive layer buried within a halfspace shows that the resistivity structure of the seafloor can be independently resolved from the cable location. Further studies of these two models also indicate that the position of the streamer must be roughly known in advance on the order of a hundred metres to be used as a suitable starting model in a non-linear inversion. The crucial information is contained in the parts of the pulse which travel through the seawater and which act as a calibration path. Such information is absent for a static DC method.

Keywords: Inverse theory; Electrical properties; Electromagnetic theory; Marine electromagnetics; Gas and hydrate systems; Composition of the oceanic crust.

1 INTRODUCTION

The controlled source electromagnetic (CSEM) method has become a popular technique to map the electrical resistivity structure of the seafloor. Geological targets such as petroleum, gas or gas-hydrate deposits, magma chambers, subduction zones, seafloor sulfides and freshwater lenses all have anomalous resistivity features and may be suitable subjects for a marine CSEM survey. Although there are several variations (e.g. Edwards *et al.* 1985; Cheesman *et al.* 1987 or Holten *et al.* 2009), the most common marine CSEM system uses a time varying horizontal electric dipole (HED) source, galvanically coupled to the seawater and seafloor. Electromagnetic fields, which are measured on the seabed by nodal or cable based dipole receivers, are sensitive to the resistivity structure of the earth. An accurate knowledge of the transmitter and receiver geometry is extremely important for proper interpretation; errors in the position and orientation of the transmitter and/or the receivers propagate into errors in the predicted seafloor resistivity. At sea, precise naviga-

tion requires the deployment of short baseline acoustic transponders with accompanying costs in both ship time and instrumentation. Is there an alternative? Are there any possible CSEM configurations that allow navigation to be determined directly from the measured data?

Previously, Weitemeyer (2008) approached this type of problem for a conventional nodal system by inverting for the positions and orientations of the transmitter and receivers along with seafloor resistivity. Similarly, Key & Lockwood (2010) inverted for the orientation of the receivers along with seafloor resistivity, but assumed that all other navigational parameters were known. Let us consider specific type of configuration. The University of Toronto marine electromagnetics group has deployed a stationary seafloor CSEM transmitter in the framework of the NEPTUNE Canada underwater cabled observatory offshore Vancouver Island. The purpose of this system is to monitor the gas-hydrate deposits known to be present in the area Mir (2011). The transmitter has a well-known position and orientation since it was deployed using a remotely operated vehicle, and is connected to and powered from the shore. Let us imagine the thought experiment of towing a cabled streamer of receivers by a ship or an autonomous underwater vehicle (AUV) in

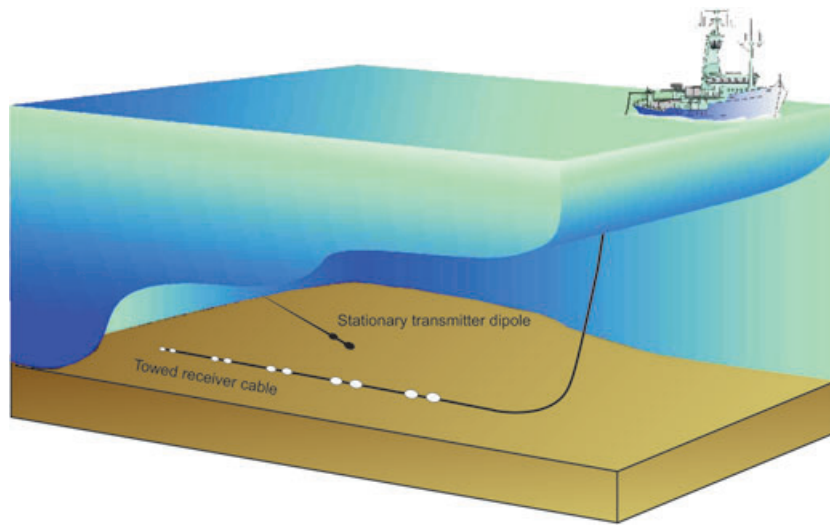*Now at: IFM-Geomar, Wischhofstrasse 1-3, 24148, Kiel, Germany.

Figure 1. Illustration of the fixed transmitter, towed receiver marine CSEM configuration.

the nearby area (Fig. 1). Although the transmitter's location and orientation are well known, the location of the towed receiver cable has to be determined. In this paper, we shall investigate the joint inversion of data from such a system to obtain both the electrical resistivity of the seafloor and the unknown navigational parameters. The orientation of the streamer may be assumed to be the same as the well-established heading of the ship or AUV. Moreover, the inter-receiver spacing is fixed by the cable length and is known with a high degree of certainty. This essentially provides information on the electric field and its gradient within a certain region of the seafloor. Clark (2009) has shown that it is possible to locate a magnetic source using measurements of both the static magnetic field and its gradient. The problem studied in our paper is much the same; since the transmitter position and orientation are known, the only remaining unknown navigational parameter is the location of the first receiver on the streamer. This paper examines the resolution properties of this inverse problem to see if the array location can be independently resolved from the seafloor resistivity structure. No doubt the inversion is non-linear. Thus the choice of starting models is also examined to establish the required quality of any available navigational data.

2 ARRAY GEOMETRY

Consider an HED transmitter of moment p, which is switched on abruptly. Assume that the dipole, situated on the seafloor, is oriented in the x-direction at the origin (Fig. 2). A streamer of N electric field receivers is towed on the seabed at an angle ϕ with respect to the source. Receiver 1 is located at position (x, y); the offset between Receiver i and Receiver $i + 1$ is denoted by r_i. The known parameters are ϕ, p, N, the location of the transmitter and each r_i. The unknown parameters are x, y and the earth resistivity structure (the seawater resistivity and depth would typically be known in advance). The electric field E_i at the ith receiver is measured inline with the cable. This field is a trigonometric combination of E_i^x and E_i^y, respectively the x and y directed fields at the receiver, and is given as

$$E_i = E_i^x \cos \phi + E_i^y \sin \phi. \tag{1}$$

For the simple case of a layered earth, E_i^x and E_i^y can be found in various works (e.g. Chave & Cox 1982, Swidinsky 2011). Given

a set of electric field data, we can invert for (x, y), the position of the first receiver, together with the seafloor resistivity structure. However, it is important to first study the effects of parameter inter-correlation for such an inverse problem. If the array location and the resistivity structure cannot be independently resolved, many of the practical advantages of the configuration are lost. Eigenparameter statistical analysis is a common way to investigate resolution properties and our style of its application is summarized briefly here. The reader is referred to Edwards (1997) for further description.

3 EIGENPARAMETER STATISTICAL ANALYSIS

The investigation of the resolution by a given data set of a model parameter has to address a fundamental question of uniqueness. When one parameter of a model is changed, a change will be observed in the model type curve, which passes through the data. If a certain parameter change moves the type curve, on average, just outside the errors on the data, it is tempting to state that the parameter is resolved to an accuracy, which depends simply on size of this change. Unfortunately, the way in which the type curve is displaced need not be unique, and varying the value of a different model parameter, or the values of a particular group of model parameters, sometimes produces a very similar displacement. In such a case, one cannot argue that the first model parameter is resolved by the data even though varying it does significantly alter the form of the type curve. The problem of this type of parameter intercorrelation is avoided by a technique known as eigenparameter statistical analysis. The method provides a very clear, unambiguous set of statements for the interpreter, or the designer, of an experiment for assessing the errors and parameter intercorrelations in a multiparameter model determined from a synthetic or real data set with associated standard errors.

Let a given model have parameters $P_j, j = 1{:}M$. The P_j are the thicknesses and resistivities of the layered model along with the navigational parameters. Let the data set, either an experimental or a synthetic one, from which the model is determined be $Y_i, i = 1{:}N$, and let the measured or assigned errors on the data be $e_i, i = 1{:}N$. For a small variation dP_j in a parameter P_j, the expected changes
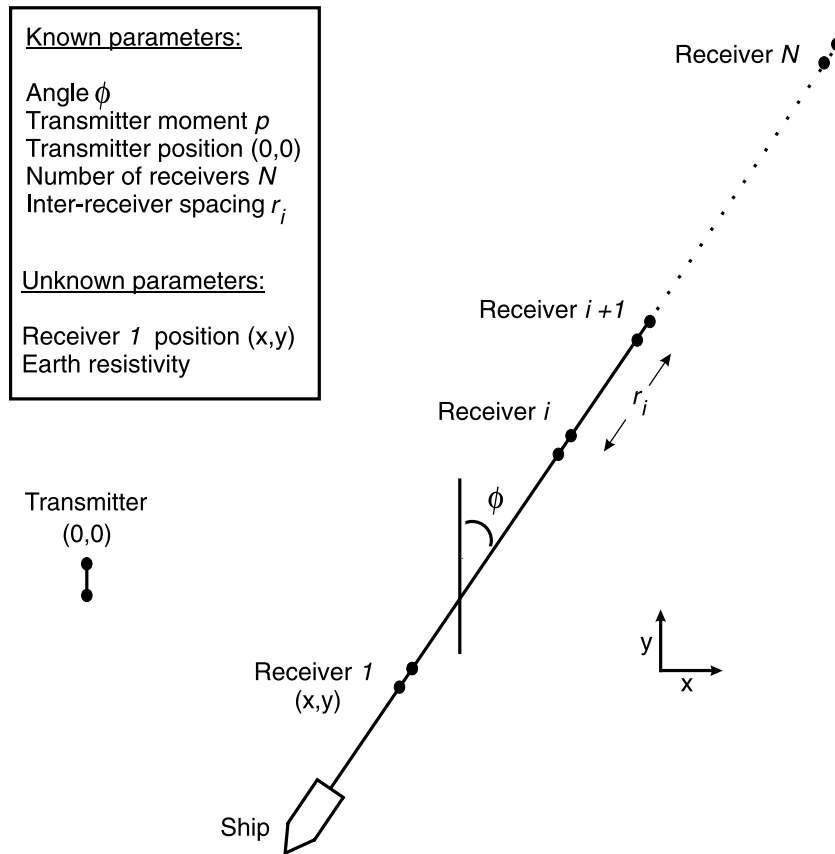
Figure 2. Survey parameters used to describe the fixed transmitter, towed receiver array in plan view. There are two unknown navigational parameters: the x and y positions of Receiver 1.

dY_i in the data set Y_i are given by the first term of Taylor's series as

$$dY_i = \sum_{j=1}^{M} A_{ij}\, dP_j \tag{2}$$

or, in matrix notation,

$$dY = A \cdot dP, \tag{3}$$

where each coefficient A_{ij} is simply a measure of the sensitivity of datum Y_i to a change in parameter P_j, or the partial derivative $\partial Y_i/\partial P_j$. These derivatives may be found either analytically or numerically from the forward solution given the physics of the problem.

Expressions (2) and (3) clearly display the problem of non-uniqueness. A given change in a datum can be produced by changing any one of the model parameters provided the associated A_{ij} is non-vanishing. However, it is possible to choose linear combinations dP^* of the parameter changes dP and corresponding linear combinations dY^* of the data changes dY such that expressions (2) and (3) are greatly simplified. The process of finding these combinations is through Singular Value Decomposition (SVD) of the matrix A. Standard software exists to write A as

$$A = U \cdot L \cdot V^{T}. \tag{4}$$

The matrices U and V have the property that

$$U^{T} \cdot U = V^{T} \cdot V = V \cdot V^{T} = I \tag{5}$$

and the matrix L is diagonal. If dY^* and dP^* are defined by the equations

$$dY^* = U^{T} \cdot dY \tag{6}$$

and

$$dP^* = V^{T} \cdot dP \tag{7}$$

then eq. (3) may be written as

$$dY^* = L \cdot dP^* \tag{8}$$

Only one set of weights U and V permits this simplification. The matrix L contains the eigenvalues of A. The vectors dY^* and dP^* are termed eigendata and eigenparameters, respectively. Each eigendatum is related to a corresponding eigenparameter and only that eigenparameter through the equation

$$dY_j^* = L_{jj} dP_j^*, \quad 1 \le j \le N. \tag{9}$$

The problem of parameter intercorrelation is clearly avoided if parameter resolution and error assessment are considered in terms of these eigensolutions.

The error in each eigenparameter is expressed very simply in terms of the above analysis provided each datum of the data set has an independent standard error estimate e_i of unity. Expression (6) is a relationship between small changes in the original data and small changes in the eigendata. The same set of weights must relate the errors in the two data types. If the original data errors are independent and of unit variance, Edwards (1997) shows that the standard errors in the eigendata are also independent and also have a value of unity. Now any small change in an eigendatum is related to a corresponding small change in an eigenparameter by eq. (9).

Hence, the standard error in an eigenparameter is just the reciprocal of the corresponding eigenvalue—a remarkably simple result.

Each element $\partial Y_i / \partial P_j$ of the Jacobian matrix A is scaled in two ways before SVD is undertaken. First, it is divided by e_i. This has the effect of rescaling the units in which the datum Y_i is measured so that its standard error is unity, as required by the theory. The element is also multiplied by P_j. This has the effect of redefining the parameter P_j as $\log P_j$, because

$$P_j \partial Y_i / \partial P_j = \partial Y_i / \partial (\log P_j). \tag{10}$$

The whole procedure of eigenparameter analysis clearly has very limited appeal if the eigenparameters cannot be identified as representing physically understandable combinations of the original model parameters. The use of logarithmic scaling of the model parameters makes this identification much like dimensional analysis. As an example, consider the model of a layer of resistivity ρ_2 and thickness d_2 buried at a depth d_1 within a host of resistivity ρ_1. A change in P_1^*, one of the four possible eigenparameters, is related to changes in the model parameters by

$$dP_1^* = V_{11}d(\log \rho_1) + V_{21}d(\log d_1) + V_{31}d(\log \rho_2) + V_{41}d(\log d_2). \tag{11}$$

The weights V_{11}, V_{21}, V_{31} and V_{41} are normalized by the SVD analysis so that the sum of their squares is unity. The physical interpretation of the eigenparameter may be deduced as

$$\rho_1^{V_{11}} d_1^{V_{21}} \rho_2^{V_{31}} d_2^{V_{41}}. \tag{12}$$

If the resistivity-thickness product of the layer is the 'physical interpretation' of the eigenparameter, then $V_{11} = V_{21} = 0$ and $V_{31} = V_{41} = 0.707$. Also, the standard error in the eigenparameter is the standard error in the logarithm of the resistivity-thickness product or, equivalently, the fractional standard error in the resistivity-thickness product itself.

The relationship between the fractional standard error in a given model parameter and the standard errors in the eigenparameters is obtained by inverting eq. (7), having noted from eq. (5) that the inverse of the matrix V^{T} is just the matrix V. A coarse upper bound on the fractional standard error in the resistivity ρ_2 in the example is given by

$$|V_{31}/L_{11}| + |V_{32}/L_{22}| + |V_{33}/L_{33}| + |V_{34}/L_{44}|, \tag{13}$$

where L_{11}, L_{22}, L_{33} and L_{44} are the eigenvalues of the Jacobian. A fractional error in a model parameter may only be computed in this manner provided it is small compared with unity because the theory described is only valid for small changes, that is to first order. If the standard error in the parameter is predicted as being much larger than unity, due for example to a non-zero weight being divided by a small eigenvalue, then a different technique has to be adopted to find the true error bound.

Results of an eigenparameter analysis of our particular problem may be displayed in a visual manner, as in Scholl & Edwards (2007). The relative weights of the original parameters contained in each eigenparameter are shown as circles the sizes of which are proportional to the weight; positive weights are shown as white circles while negative weights are shown as black circles. Since we use the logarithm of the original parameters as components of the eigenparameters, an eigenparameter composed, for example, of a black and white circle of roughly equal size corresponds to a difference of the two log-parameters, and consequently to a quotient of the original parameters.

Consider a simple model consisting of a halfspace underneath a water column (Fig. 3a). The earth and survey parameters are given in the figure caption. Let us assume that the depth and resistivity of the seawater is known *a priori*, while the resistivity of the seafloor is unknown. Here there are three unknown parameters: The resistivity of the seafloor and the x and y position of the first receiver. Fig. 4 shows the results of an eigenparameter analysis for this case. The first two eigenparameters are mainly composed of the navigational parameters, while the third eigenparameter is mainly composed of the seafloor resistivity. It is clear from the decoupling behaviour of these two simple situations that the seafloor structure can be independently resolved from the array location. Assuming a 1 per cent error on each electric field measurement along the transient response, the seafloor resistivity and the position of the array can be established to an error of much less than 1 per cent.

Next, consider a model consisting of a resistive layer embedded in a halfspace host (Fig. 3b). The survey parameters are given in the figure caption. Let us assume that the depth and resistivity of the seawater, the depth to the layer and the host resistivity are known *a priori*, while the resistivity and thickness of the layer are the unknown parameters. This situation is similar to the case of the gas-hydrate deposits under observation by NEPTUNE Canada, where the properties of the resistive target are not only unknown but are in fact believed to be changing over time, while the depth to the target and the host properties have been well established through previous studies (e.g. Hyndman *et al.* 2001, Riedel *et al.* 2002). In this case there are four unknown parameters: The resistivity and thickness of the layer, and the x and y position of the first receiver. Fig. 5(a) shows the results of an eigenparameter analysis for this case. The first and second eigenparameters are composed of mainly navigational parameters, while the third and fourth eigenparameters are composed of mainly earth parameters. Again, it is clear from this decoupling behaviour that the resistive target can be independently resolved from the array location. Assuming a 1 per cent error on each electric field measurement along the step-on response, the position of the array can be established to an error of much less than 1 per cent. However, note that the resistivity and thickness of the layer cannot be well-resolved independently; as expected, only their product may be found with a reasonable error of approximately 1 per cent, while their quotient, (the conductivity-thickness product), has a much higher error. As a check, Fig. 5(b) shows the results of an eigenparameter analysis where the navigational parameters are known. Again, the resistivity-thickness product can be found with a low error, while the conductivity-thickness product cannot. Note that in this case, the errors are lower than the cases where the navigational parameters are unknown, as one would expect.

Finally, consider again the model consisting of a resistive layer embedded in a halfspace host. However, in this case, let all earth parameters be unknown, while the depth and resistivity of the seawater are still known *a priori*. In this case there are six unknown parameters: The resistivity of the host, the resistivity, thickness and depth of the layer and the x and y position of the first receiver. Fig. 6(a) shows the results of an eigenparameter analysis for this case. The first and second eigenparameters is composed of mainly navigational parameters, while the third, fourth, fifth and sixth eigenparameters are composed of only earth parameters. In both cases, note that the earth eigenparameters are mainly divided into combinations of the host resistivity and the layer depth, and combinations of the layer thickness and resistivity, as one might expect. Again, the resistivity-thickness product of the resistive layer can be found with a low error,
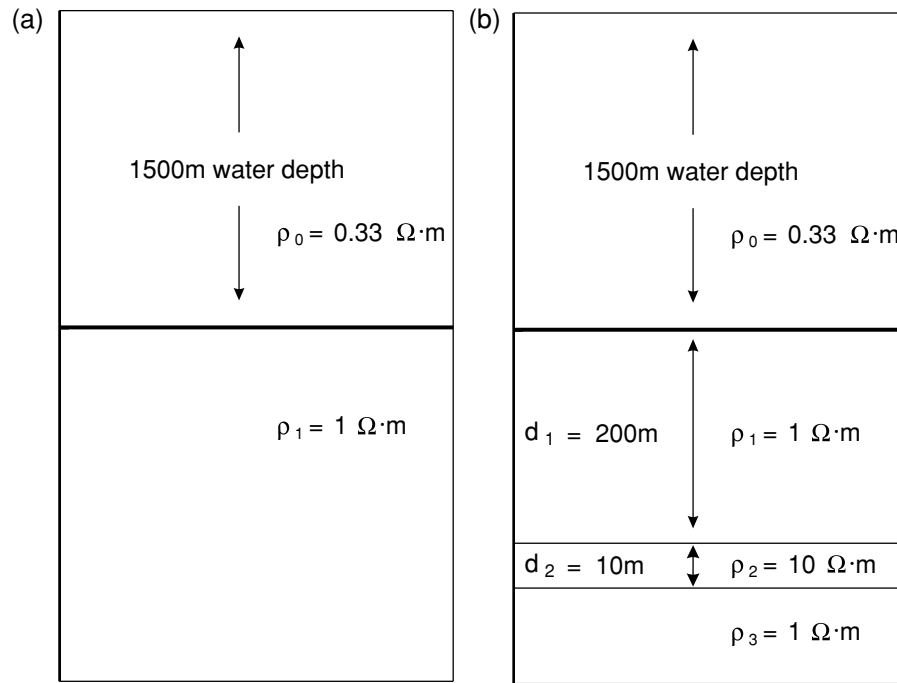
Figure 3. (a) The halfspace model used in this study. The survey parameters used are $\phi = 15^{\circ}$, $N = 5$, $p = 100\,kA\,m$, $x = 200\,m$, $y = 200\,m$, each interreceiver spacing $= 100\,m$, 21 times ranging logarithmically from 0.03 s to 30 s, and a 1 per cent standard deviation on the measured data, as might be found through pre-processing and stacking of raw transients over many cycles. (b) The layered model used in this study. All other parameters are the same as described in the caption of (a).
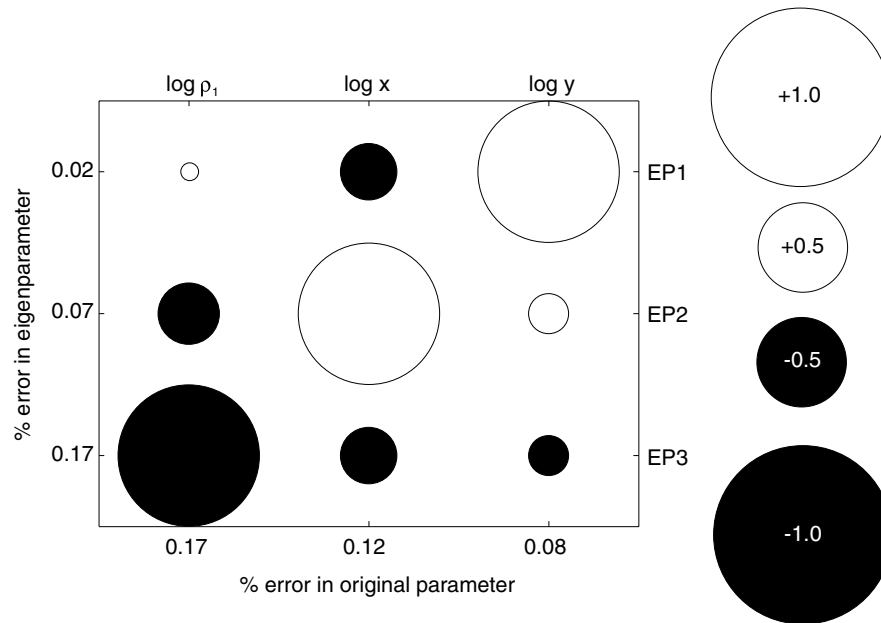

Figure 4. Resolution analysis for the halfspace model in Fig. 3(a). The white circles are positive components of each eigenparameter (EP) while black circles are negative. The size of each circle corresponds to the magnitude of each contribution. The values along the LH column correspond to the percent error for each eigenparameter, while the values at the bottom correspond to the percent error for each original parameter. The seawater depth and resistivity are assumed known.

while the conductivity-thickness product cannot. The analysis again shows that seafloor structure can be independently resolved from the array location and we see that the position of the array can be established to an error of much less than 1 per cent. As a check,

Fig. 6(b) shows the results of an eigenparameter analysis where all navigational parameters are known, but all earth parameters are not. We can see that the earth eigenparameters are divided into roughly the same combinations as the case when the navigational parameters
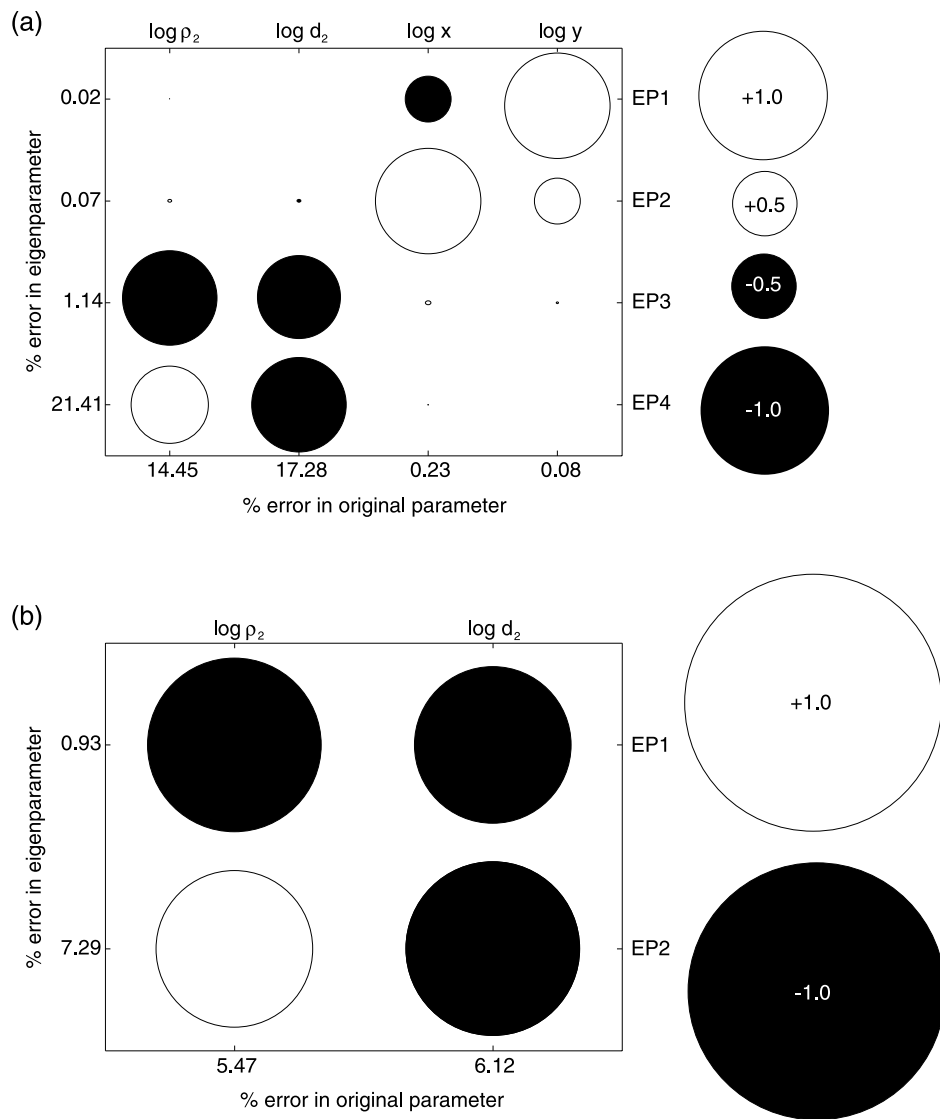
Figure 5. Resolution analysis for the layered model in Fig. 3(b). (a) The seawater depth and resistivity, the host resistivity and the depth to the resistive layer are assumed known. (b) All navigational parameters, the seawater depth and resistivity, the host conductivity and the depth to the resistive layer are assumed known.

are unknown. Similarly with the results shown in Fig. 5, the errors are lower than the case where there are more unknowns.

4 ANALYSIS OF NON-LINEAR EFFECTS

In the previous section, the analysis was conducted assuming the true earth model. However, since the electromagnetic inverse problem is non-linear, it is also important to examine how the choice of starting models will affect the final result. We use the non-linear inversion technique, downhill simplex (Neader & Mead 1965), also known as Amoeba, to invert synthetic test data. Amoeba creates a polygon with $M + 1$ vertices in an M dimensional model space, where a different choice of unknown parameters makes up each vertex. The misfit at each vertex is calculated, and vertices are reflected, expanded, contracted and reduced around the simplex until the desired misfit is obtained. The advantages of using Amoeba are twofold: Derivatives are not required and a choice of multiple start-

ing models must be used as input. The latter benefit is particularly useful in the present scenario as the survey operator should have some knowledge of the streamer location. The initial simplex may be constructed by using a rough, but intelligent guess of the region within which the cable is believed to lie. In comparison, Weitemeyer (2008) uses a Marquardt technique to invert for the seafloor resistivity together with the transmitter position, the transmitter dipole antenna rotation and dip, and the positions and orientations of the nodal receivers (all potentially unknown navigational parameters for a conventional nodal system). A single model is guessed at the start of the process, as required by the linearization employed in the Marquardt inversion.

Consider the model given in Fig. 3(b). Assume that the host resistivity and the depth to the layer is known, so that $M = 4$ and we have $M + 1 = 5$ different starting models. Table 1 shows the results of a downhill simplex inversion of synthetic data contaminated with 1×10^{-7} V m^{-1} Gaussian noise. The starting models and the final result with an RMS misfit of 2.75 are given in Table 1, showing that
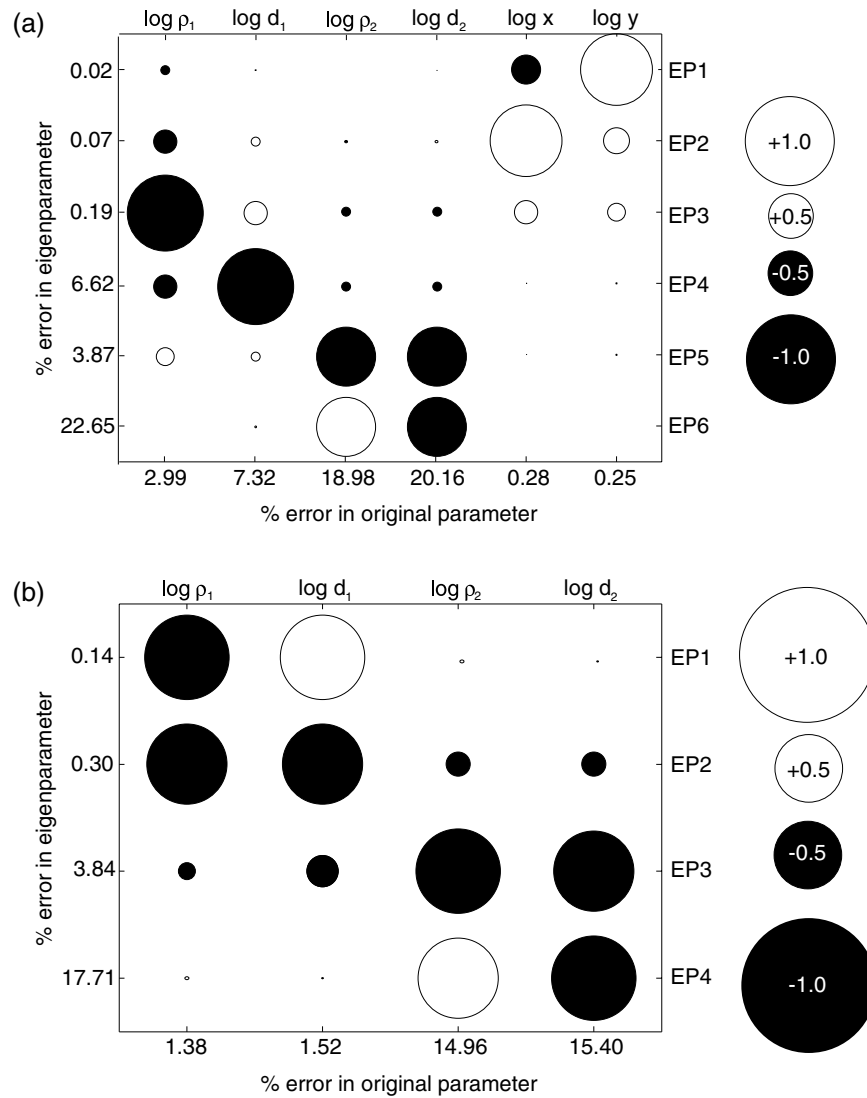
Figure 6. Resolution analysis for the layered model in Fig. 3(b). (a) The seawater depth and resistivity are assumed known while all earth parameters are unknown. (b) All navigational parameters, the seawater depth and resistivity are assumed known while all earth parameters are unknown.

Table 1. Results from inversion of synthetic data for the situation in Fig. 3(b). The seawater depth and resistivity, the host resistivity and the depth to the resistive layer are assumed known.

	Starting model for Amoeba					Inversion result (RMS = 2.75)
x (m)	300	100	300	100	300	201.4
y (m)	300	300	100	100	300	200.2
d_2 (m)	5	5	5	25	25	13.1
ρ_2 (Ω m)	2	2	2	20	20	8.3

a navigational uncertainty of approximately 100 m is acceptable as a suitable starting model. Since the resistivity and thickness of the thin layer cannot be independently resolved, note that the individual parameters found by the inversion ($\rho_2 = 8.3$ Ω m, $d_2 = 13.09$ m) are not the same as the original model ($\rho_2 = 10$ Ω m, $d_2 = 10$ m). However, the resistivity-thickness product found by the inversion (109 Ω m^2) is close to the truth (100 Ω m^2), as expected from the

eigenparameter analysis. Fig. 7 compares the modelled inversion result with the noisy synthetic data for all five receivers, showing that the two curves agree well.

Now, consider a somewhat more complicated situation. Let all earth parameters in Fig. 3(b) be unknown, and let the vessel tow the array through five waypoints so that $M = 14$ and we have $M + 1 = 15$ different starting models. The grey region in Fig. 8(a) shows raw, synthetic data from such a survey, in this case having 10 per cent standard error (as illustrated by the thickness of the line), but no additional noise. The black line shows the modelled data from the downhill simplex inversion of this synthetic data, indicating that the two curves agree well. Fig. 8(b) shows the actual path of the vessel along with the reconstructed path of the vessel for a downhill simplex inversion assuming either small (3 per cent) or large (10 per cent) errors in the synthetic data. The search region used to select starting models for the inversion process is shown on the map as a grey rectangle. The navigational parameters for the 15 starting models are selected randomly from this region. Observe that the
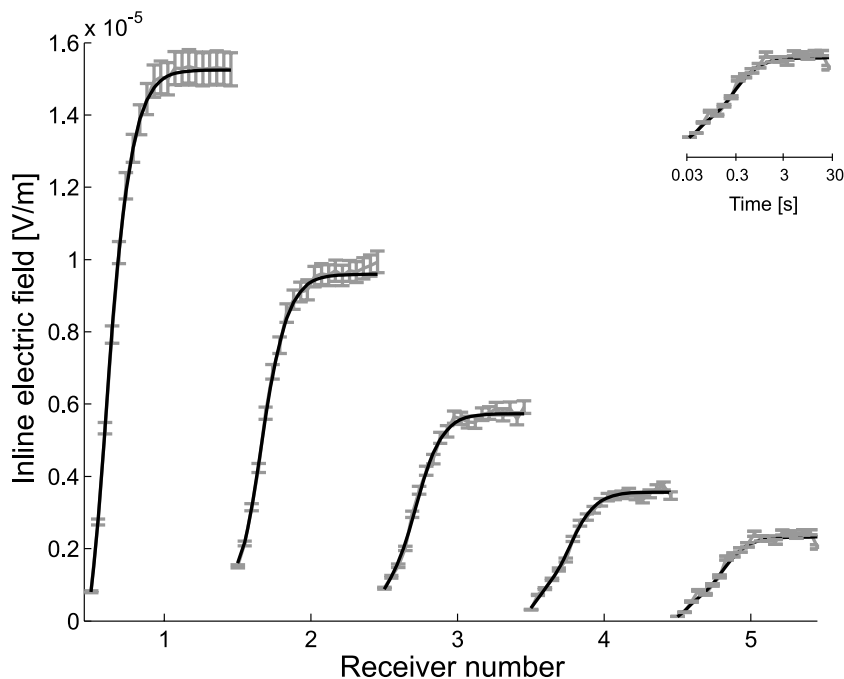
Figure 7. Raw data and modelled results from the inversion of synthetic data for the model in Fig. 3(b). The seawater depth and resistivity, the host resistivity and the depth to the resistive layer are assumed known. The black line shows the inversion result while the grey error-bars show the original synthetic data with 3 per cent standard deviation. Gaussian noise with a mean of 1E-7 *V/m* was added to the synthetic data to represent systematic errors not removed by stacking. 40 iterations of Amoeba were required to obtain the fit. For clarity, the timescale is not shown on the horizontal axis, but the transients sweep logarithmically in time from 0.03 s to 30 s for each receiver. The inset shows the step-response of Receiver 5 with a timescale as an example.

reconstructed vessel track is very close to the true path, even for the case of high error. Table 2 shows the earth parameters obtained from this inversion process for the two different error levels. Also shown in Table 2 is the range of starting models for the earth parameters used in the inversion. The earth parameters for the 15 starting models are selected randomly within these ranges. Amoeba required 49 iterations for the 3 per cent error model and 24 iterations for the 10 per cent error model. We see that in both the low and high error cases, the inversion results are very similar to the true model, but of course are worse for the case with higher error. Note that the inverted resistivity-thickness product of the resistive layer is close to the original model, although the individual parameters are not. From this somewhat more complicated scenario, it is again clear that the navigational parameters may be estimated with an uncertainty of approximately 100 m to be used as a suitable starting model for an inversion.

5 CONCLUSIONS

Using a marine CSEM configuration consisting of a stationary transmitter and a towed receiver cable, navigation and seafloor resistivity may be determined independently. For our particular example, the position of the cable must be known *a priori* on the order of roughly a 100 m. Such a level of accuracy should be possible using simple trigonometric arguments based on the amount of cable deployed and its tilt off the stern of the survey vessel. However, this uncertainty range may vary depending on factors such as the cable position and orientation, the earth model, the model parameterization, the particular inversion method and the noise level. This implies that for every case the range of acceptable navigational uncertainty should be carefully examined prior to a survey. The synthetic inversions

are oversimplified; a more proper 1-D inversion would divide the unknown earth model into many layers, yielding many more unknown parameters (e.g. Constable *et al.* 1987, Key 2009). However, the principle results should remain the same. The effects of 3-D targets remain unexamined. Such structures will undoubtedly distort the fields, but may be treated by full 3-D inversion. It is speculated that even the most complicated models should exhibit the same decoupling behaviour as long as the seawater depth and resistivity is known; this *a priori* information provides a calibration path through which the electromagnetic fields travel. It should be noted that the decoupling observed in this model study will not necessarily occur at all cable positions and orientations; consider, for example, that when $x \sim 0$ m, and $\phi \sim 90°$, there will be a null calibration field through the seawater. For this reason an eigenparameter analysis should always be performed during a survey design stage. Even though the HED source has been shown to have superior resolution (Key 2009), it is further speculated that additional field components will further improve the inversions, especially for 3-D structures (additional transmitter components would be far easier to implement than receiver components in practice due to the stationary nature of the source). The next logical step would then be to investigate the effects of vertical electric dipole sources along with magnetic dipole sources. The concern that the receiver cable may not lie straight on a seafloor with rough bathymetry may be overcome by using a neutrally buoyant streamer.

Our proposed configuration may have applications other than the NEPTUNE Canada observatory. For example, it could be used for production monitoring of oil and gas operations; one or more transmitters could be connected to a nearby drilling platform and tow lines could be altered from survey to survey depending on the
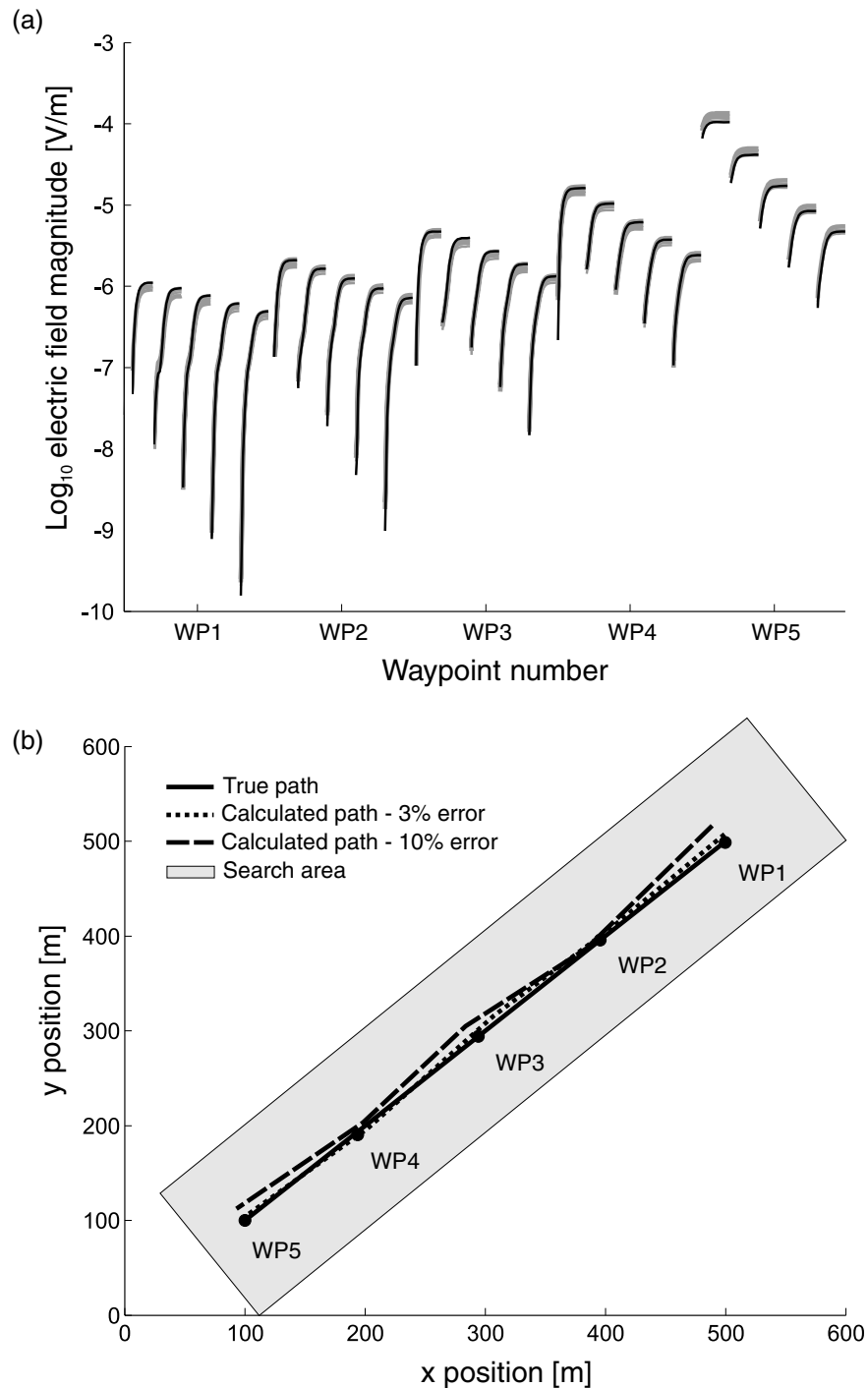
Figure 8. (a) Synthetic data and modelled results from the inversion for the model in Fig. 3(b) with the array passing through multiple waypoints. The seawater depth and resistivity are assumed known while all earth parameters are unknown. The black line shows the inversion result while the grey line shows the original synthetic data, in this case with 10 per cent standard deviation as illustrated by the thickness of the line. For clarity, the timescale is not shown on the horizontal axis, but the transients sweep logarithmically in time from 0.03 s to 30 s for each receiver at each waypoint. For each transient, the timescale is the same as shown in the inset in Fig. 7. No additional noise was added to the synthetic data. Note the log scale on the *y*-axis, in contrast to Fig. 7. (b) Reconstructed vessel track for the synthetic data shown in (a). The original path, and the inverted path for synthetic data with 3 per cent error and 10 per cent error are shown on the map. The search region used to select starting models for the inversion process is shown on the map as a grey rectangle. The discrete waypoints of the original path are shown as dots. The transmitter is at the origin and has a moment of 100 kA m. The inter-receiver spacing is 100 m.

state of the reservoir. We also speculate that the analysis should carry over to several other CSEM configurations and geometries, such as a stationary receiver array with a towed transmitter (Swidinsky & Edwards 2011). It may also be relevant in the search for submarines

and other manmade objects, which act as electrical sources. In this case, the receiver array would be located on the seafloor and its position would be well known, while the source location, source strength and earth resistivity structure would not.

Table 2. Results from inversion of synthetic data from the model in Fig. 3(b) given multiple waypoints. The seawater depth and resistivity are assumed known while all earth parameters are unknown. Results for two different noise models are shown.

	True model	Starting model range	Inversion result 3 per cent error (RMS = 1.59)	Inversion result 10 per cent error (RMS = 0.90)
d_1 (m)	200	190–210	201.0	201.5
ρ_1 (Ω m)	1	0.5–2	0.86	1.27
d_2 (m)	10	1–20	14.2	4.8
ρ_2 (Ω m)	10	1–100	6.8	25.7

ACKNOWLEDGMENTS

REFERENCES

Chave, A.D. & Cox, C.S., 1982. Controlled electromagnetic sources for measuring the electrical conductivity beneath the oceans, *J. geophys. Res.,* **87,** 5327–5338.

Cheesman, S.J., Edwards, R.N. & Chave, A.D., 1987. On the theory of sea-floor conductivity mapping using transient electromagnetic systems, *Geophysics,* **52,** 204–217.

Clark, D., 2009. Magnetic Tensor Gradiometry in the Marine Environment: correction of electric and magnetic field and gradient measurements in a conductive medium and improved methods for magnetic target location using the magnetic gradient tensor, in *Proceedings of the 2009 MARELEC Conference,* Stockholm.

Constable, S.C., Parker, R.L. & Constable, C.G., 1987. Occam's inversion:

a practical algorithm for generating smooth models from electromagnetic sounding data, *Geophysics,* **52,** 289–300.

Edwards, R.N., 1997. On the resource evaluation of marine gas hydrate deposits using a sea floor transient electric dipole–dipole method, *Geophysics,* **62,** 63–74.

Edwards, R.N., Law, L.K., Wolfgram, P.A., Nobes, D.C., Bone, M.N., Trigg, D.F. & DeLaurier, J.M., 1985. First results of the MOSES experiment: sea sediment conductivity and thickness determination, Bute Inlet, British Columbia, by magnetometrlc offshore electrical sounding, *Geophysics,* **50,** 153–161.

Holten, T., Flekkøy, E.G., Singer, B., Blixt, E.M., Hanssen, A. & Måløy, K.J., 2009. Vertical source, vertical receiver, electromagnetic technique for offshore hydrocarbon exploration, *First Break,* **27,** 89–93.

Hyndman, R.D., Spence, G.D., Chapman, R., Riedel, M. & Edwards, R.N., 2001. Geophysical studies of marine gas hydrate in Northern Cascadia. *Geol. Surv. Canada geophys. Monogr.,* 273–295.

Key, K., 2009. 1D inversion of multicomponent, multifrequency marine CSEM data: methodology and synthetic studies for resolving thin resistive layers, *Geophysics,* **74,** F9–F20.

Key, K. & Lockwood, A., 2010. Determining the orientation of marine CSEM receivers using orthogonal Procrustes rotation analysis, *Geophysics,* **75,** F63–F70.

Nelder, J. A. & Mead, R., 1965. A simplex method for function minimization, *Comput. J.,* **7,** 308–313.

Mir, R., 2011 Design and deployment of a controlled source EM instrument on the NEPTUNE observatory for long-term monitoring of methane hydrate deposits, *PhD thesis*, University of Toronto.

Riedel, M., Spence, G.D., Chapman, N.R. Hyndman, R.D., 2002. Seismic investigations of a vent field associated with gas hydrates, offshore Vancouver Island. *J. geophys. Res.,* **107,**(B9), 2200, doi:10.1029/2001JB000269.

Scholl, C. & Edwards, R.N., 2007. Marine downhole to seafloor dipole-dipole electromagnetic methods and the resolution of resistive targets, *Geophysics,* **72,** WA39–WA49.

Swidinsky, A., 2011. Transient electromagnetic modelling and imaging of thin resistive targets: applications for gas-hydrate assessment, *PhD thesis*, University of Toronto.

Swidinsky, A. & Edwards, R.N., 2011. Navigation and resistivity inversion using stationary seafloor instruments, in *Proceedings of the 2009 MARELEC conference*, San Diego.

Weitemeyer, K., 2008. Marine electromagnetic methods for gas hydrate characterization, *PhD thesis*, University of California, San Diego.